crystals

MDPI

Article

Frustrated Magnet $Mn_3Al_2Ge_3O_{12}$ Garnet: Crystal Growth by the Optical Floating Zone Method

Manisha Islam [1,*], Monica Ciomaga Hatnean [1,2,3], Geetha Balakrishnan [1] and Oleg A. Petrenko [1]

[1] Department of Physics, University of Warwick, Coventry CV4 7AL, UK
[2] Laboratory for Multiscale Materials Experiments, Paul Scherrer Institute (PSI), 5232 Villigen, Switzerland
[3] Materials Discovery Laboratory, Department of Materials, ETH Zurich, 8093 Zurich, Switzerland
* Correspondence: manisha.islam@warwick.ac.uk

Abstract: $Mn_3Al_2Ge_3O_{12}$ is a member of the garnet family of compounds, $A_3B_2(CO_4)_3$, whose magnetic properties are affected by a high degree of geometrical frustration. The magnetic frustration is at the origin of the intriguing magnetic properties that these materials exhibit, such as a long range *hidden order* derived from multipoles formed from 10-spin loops in the gadolinium gallium garnet, $Gd_3Ga_5O_{12}$. $Mn_3Al_2Ge_3O_{12}$ garnet is isostructural to the thoroughly investigated Gd garnets, $Gd_3Ga_5O_{12}$ and $Gd_3Al_5O_{12}$. Moreover, in $Mn_3Al_2Ge_3O_{12}$, the Heisenberg-like Mn^{2+} magnetic ions ($L = 0$) are also arranged in corner sharing triangles that form a hyperkagomé structure. The identical crystallographic structures and similar Heisenberg-like behaviour of the magnetic ions make manganese aluminium germanium garnet the closest compound to the gadolinium garnets in its magnetic properties. Here, we report, for the first time, the growth of a large, high quality single crystal of the $Mn_3Al_2Ge_3O_{12}$ garnet by the floating zone method. X-ray diffraction techniques were used to characterise and confirm the high crystalline quality of the $Mn_3Al_2Ge_3O_{12}$ crystal boule. Temperature-dependent magnetic susceptibility measurements reveal an antiferromagnetic ordering of the Mn^{2+} ions below $T_N = 6.5$ K. The high quality of the single crystal obtained makes it ideal for detailed investigations of the magnetic properties of the system, especially using neutron scattering techniques.

Keywords: crystal growth; floating-zone technique; garnets; frustrated magnet

Citation: Islam, M.; Ciomaga Hatnean, M.; Balakrishnan, G.; Petrenko, O.A. Frustrated Magnet $Mn_3Al_2Ge_3O_{12}$ Garnet: Crystal Growth by the Optical Floating Zone Method. *Crystals* **2023**, *13*, 397. https://doi.org/10.3390/cryst13030397

Academic Editor: Ludmila Isaenko

Received: 27 January 2023
Revised: 17 February 2023
Accepted: 23 February 2023
Published: 25 February 2023

1. Introduction

The garnet family of compounds is characterised by the general formula $A_3^{2+}B_2^{3+}(C^{4+}O_4)_3$ [1–3] where A, B and C sites are occupied by divalent, trivalent and tetravalent cations. The manganese-containing garnets have a cubic crystal structure, belonging to the $Ia\bar{3}d$ space group. The magnetic Mn ions are positioned on the A site, forming two interpenetrating hyperkagomé lattices in which the magnetic ions are arranged in corner sharing triangles. These adjacent triangles lie with an angle of 73.2° between them, creating a three dimensional structure [4]. The antiferromagnetically coupled ions on the triangular lattice facilitate geometric magnetic frustration, prompting interest in the garnet structure.

Geometric frustration arises when a system is unable to minimise the competing interactions due to its crystallographic structure, preventing a single ground state to be favoured [5–7]. Magnetic frustration is usually a consequence of neighbouring moments interacting so that a large ground state degeneracy is achieved, suppressing long range order, giving rise to rich and exotic magnetic behaviour, such as glassy, spin liquid [8], spin-orbital-entangled liquid [9] and spin ice [10] phases. As a result, systems containing edge and corner-sharing triangular arrangement of antiferromagnetically interacting spins are of great interest in the field of frustrated magnetism. The most established systems exhibiting this kind of magnetic structure are pyrochlores [11], garnets [12] and kagomé [13,14] lattices.

The gadolinium gallium garnet (GGG), $Gd_3Ga_5O_{12}$, has been extensively studied as the archetypal frustrated magnet [4,15–17]. GGG displays no long-range magnetic order in zero-field despite its relatively strong antiferromagnetic correlations. Diffuse neutron scattering patterns with a distinct Q-dependence displayed by both polycrystalline and single crystal samples of GGG have been interpreted as evidence for a long-range *hidden magnetic order*.

This new director state is derived from the three dimensional triangular arrangement of localised spins and the corresponding perturbative magnetic anisotropy, with the directors localised to the centre of 10-spin loops of the Gd ions [16]. Recent results on gadolinium auminium garnet (GAG) have also piqued interest as a candidate for the 10-spin loop director state [4]. Despite the high theoretical interest in GGG and GAG, the prohibitively high neutron absorption cross section of the Gd isotopes makes it extremely hard to experimentally probe the magnetic structure of Gd compounds using neutron scattering techniques.

The crystal structure of $Mn_3Al_2Ge_3O_{12}$ (MAGG) is identical to that of GGG, while the magnetic structure is comprised of Heisenberg-like magnetic ions $Mn^{2+}(L = 0)$. These characteristics make $Mn_3Al_2Ge_3O_{12}$ the closest compound to GGG in its magnetic properties, being a strong candidate for exhibiting the *hidden magnetic order*, previously observed in GGG. The significantly lower neutron absorption of the constituent magnetic Mn^{2+} ions, relative to the Gd ions, is advantageous for neutron scattering techniques.

Figure 1 illustrates the crystal structure of $Mn_3Al_2Ge_3O_{12}$. The Mn^{2+} cations on the triangular lattice form a hyperkagomé structure while the Al^{3+} cations occupy the *B* sites and the Ge^{4+} cations occupy the *C* sites.

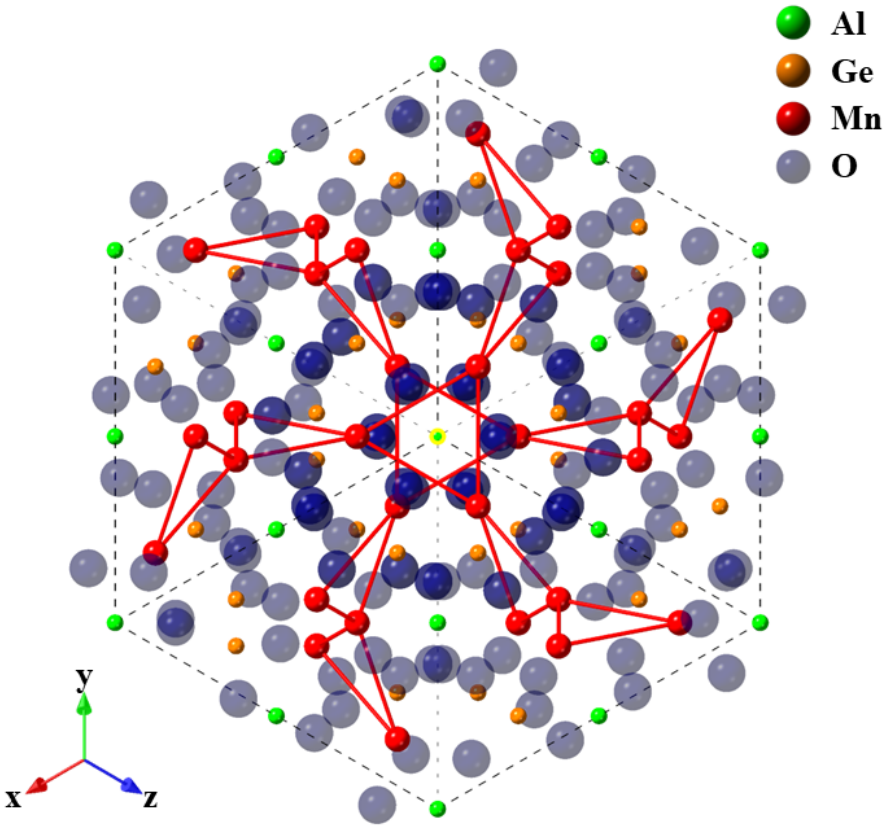

Figure 1. Crystal structure of $Mn_3Al_2Ge_3O_{12}$. The Mn-Mn "bonds" highlighted in red emphasize the formation of a hyperkagomé structure. The cubic unit cell is viewed along the [111] direction and outlined using black dashed lines.

A rhombohedral magnetic structure, of magnetic space group ($R\bar{3}'c$), was first proposed for $Mn_3Al_2Ge_3O_{12}$ by Plumier [18] and Prandl [1] based on neutron diffraction

experiments in 1973. The magnetic moments of the manganese ions are oriented parallel to the [111] plane, and are directed either opposite or along the [211], [121], and [112] axes, creating a non-collinear magnetic structure with 12-sublattice antiferromagnetic ordering, slightly differing from the triangular 120° structure. This was in agreement with further studies of the magnetic properties and specific heat measurements by Valyanska et al. [19]. $Mn_3Al_2Ge_3O_{12}$ has also recently been shown to display the first order magnetoelectric effect, which is rare for a garnet and is promising for future applications [20].

For a detailed understanding of the magnetic neutron diffuse scattering signal, a sufficiently sized single crystal is required. Synthesis of $Mn_3Al_2Ge_3O_{12}$ polycrystalline material has been previously reported [21,22], as well as the growth, by the Czochralski method, of single crystals. $Mn_3Al_2Ge_3O_{12}$ single crystals of $1.5 \times 1.5 \times 1.5$ mm^3 were grown, in air, using a platinum crucible [23]. Nevertheless, to the best of our knowledge, no detailed report on the growth of large single crystals of $Mn_3Al_2Ge_3O_{12}$ is available to date, despite previous studies of the magnetic properties of this compound using single crystal samples [19,24–26].

An ideal method for the production of a relatively large and high quality crystal is the optical floating zone (FZ) technique. The lack of crucible or flux prevents contamination, making a high-purity sample, well-suited for neutron scattering and magnetic characterisation. The FZ method has been previously employed by us to successfully grow a range of single crystal frustrated magnets for detailed investigation via neutron scattering [27–30].

We have successfully prepared, for the first time, using the optical floating zone method, crystals of $Mn_3Al_2Ge_3O_{12}$ garnet. The growth of large high quality single crystals of this garnet opens up the route for detailed studies of the magnetic behavior of this frustrated magnet. This will allow the opportunity to determine the magnetic ground state of $Mn_3Al_2Ge_3O_{12}$ and to shed light on the possibility of the existence of a *hidden magnetic order* in this compound.

2. Materials and Methods

The starting materials for the synthesis of $Mn_3Al_2Ge_3O_{12}$ polycrystalline samples were MnO (99.999% purity), GeO_2 (99.998%) and Al_2O_3 (99.99%). The starting GeO_2 powder was sintered in air at 800 °C overnight to remove the moisture prior to the synthesis of the polycrystalline material. Crystals of the manganese aluminium germanium garnet, $Mn_3Al_2Ge_3O_{12}$, were then grown using a four-mirror halogen arc lamp (0.5 kW) optical image furnace (CSI FZ-T-10000-H-IV-VPS, Crystal Systems Incorporated, Hokuto, Japan).

The crystal quality of the boules was investigated using a backscattering X-ray Photonic-Science Laue camera system. A 3 cm long single crystal was isolated from the crystal boule showing the best crystalline quality. Phase purity analysis was carried out using powder X-ray diffraction (PXRD) measurements of ground fragments of the crystal. Room temperature diffractograms were collected on Pananalytical X-ray diffractometers using CuKα_1 and CuKα_2 radiation ($\lambda_{K\alpha1} = 1.5406$ Å and $\lambda_{K\alpha2} = 1.5444$ Å), over an angular range of 10–100° in 2θ, with a step size of 0.013132°. Profile refinement was performed using the FullProf software suite [31].

Chemical composition analysis was carried out by energy dispersive X-ray spectroscopy (EDAX) using a scanning electron microscope on small fragments isolated from the crystal boules.

Magnetic susceptibility measurements as a function of temperature were taken on ground fragments of the crystal, as well as on a small crystal fragment, down to 1.8 K in an applied field of 500 Oe, using a Quantum Design Magnetic Property Measurements System MPMS-5S Superconducting Quantum Interference Device (SQUID) magnetometer, SD, USA.

3. Results and Discussion

3.1. Polycrystalline Synthesis

Samples were first prepared in polycrystalline form by solid state reaction. Previous studies on other mixed oxides containing germanium [32,33] noted that Ge can be lost during the synthesis process, due to the evaporation of GeO_2 at high temperature. To overcome this drawback, one can prepare Ge-based oxide compounds using starting powder mixtures enriched in germanium. Therefore, in a first attempt, we prepared three samples (labeled MAGG_1, MAGG_2, and MAGG_3) starting with stoichiometric amounts of MnO and Al_2O_3 and different amounts of excess GeO_2 (5, 10, and 15% respectively). The oxide powders were mixed together, pressed into pellets to facilitate the chemical reaction (2 g of end material was prepared), and then heat treated in nitrogen gas atmosphere for 24 h, at 900 °C, 1100 °C and subsequently at 1150 °C. Between each synthesis step, the mixtures were thoroughly ground to ensure good homogeneity and re-pressed into pellets. Analysis of the X-ray diffraction patterns (see Figure 2a–c) collected at room temperature on the samples prepared starting with a powder mixture enriched in Ge, MAGG_1, MAGG_2, and MAGG_3, indicates that the main phase is $Mn_3Al_2Ge_3O_{12}$. Nevertheless, there are several Bragg peaks that could not be indexed with the cubic ($Ia\bar{3}d$) space group and arise due to the presence of orthorhombic (*Pbca*) $MnGeO_3$ [34] and trigonal GeO_2 ($P3_221$) impurities [35]. A larger amount of polycrystalline material was prepared using the same synthesis conditions as sample MAGG_3 and the resulting powder mixture was isostatically pressed into a cylindrical rod (5 mm diameter and 63 mm long) and sintered at 1150 °C for a further 24 h. The annealed rod was used for the crystal growth attempts.

The three samples prepared using starting powder enriched in germanium, MAGG_1, MAGG_2, and MAGG_3, contain the same impurities, despite using different amounts of excess GeO_2. Furthermore, the presence of unreacted trigonal GeO_2 ($P3_221$) hints at the possibility of preparing polycrystalline $Mn_3Al_2Ge_3O_{12}$ samples using a starting stoichiometric powder mixture. To investigate this hypothesis, a fourth sample was prepared (sample labeled MAGG_4), for which powders of the starting oxides were weighed in stoichiometric amounts and mixed together thoroughly. The resulting powder mixture was then heated in nitrogen gas atmosphere for 48 h, at 900 °C, and subsequently at 1050 °C for 48 h and 1150 °C for 72 h. The annealed mixture was reground between each step of the synthesis to ensure good homogeneity and to facilitate the reaction of the precursors. The PXRD pattern (see Figure 2d) collected at room temperature on the resulting $Mn_3Al_2Ge_3O_{12}$ powder mixture indicates that the main phase is the desired $Mn_3Al_2Ge_3O_{12}$ garnet phase. Nevertheless, there are several Bragg peaks that could not be indexed with the cubic $Ia\bar{3}d$ space group. These Bragg peaks are attributed to the presence of orthorhombic (*Pbca*) $MnGeO_3$ and rhombohedral ($R\bar{3}c$) Al_2O_3 [36] impurities. In a subsequent synthesis attempt, the duration of each synthesis step was reduced to 24 h to prevent the formation of the orthorhombic $MnGeO_3$ impurity, which forms at high temperature in atmospheric pressure when using an extended synthesis duration [33].

In a third attempt (sample labeled MAGG_5), stoichiometric amounts of MnO, GeO_2, and Al_2O_3 powders were mixed together thoroughly. The powder mixture was heat treated in nitrogen gas atmosphere for 24 h, at 900 °C, 1100 °C and subsequently at 1150 °C. The PXRD pattern obtained for the MAGG_5 sample is shown in Figure 3. An analysis of the pattern reveals the presence of mainly $Mn_3Al_2Ge_3O_{12}$ garnet phase. Nevertheless, there are a few impurity peaks that belong to the cubic ($Fd\bar{3}m$) Mn_2AlO_4 [37] and orthorhombic (*Pnma*) MnO_2 [38] phases. The sintered material was isostatically pressed into cylindrical rods and sintered at 1150 °C for a further 24 h. The impurities persisted in the rod despite the additional heat treatment step. The resulting rods were used as feed rods for the crystal growth attempts.

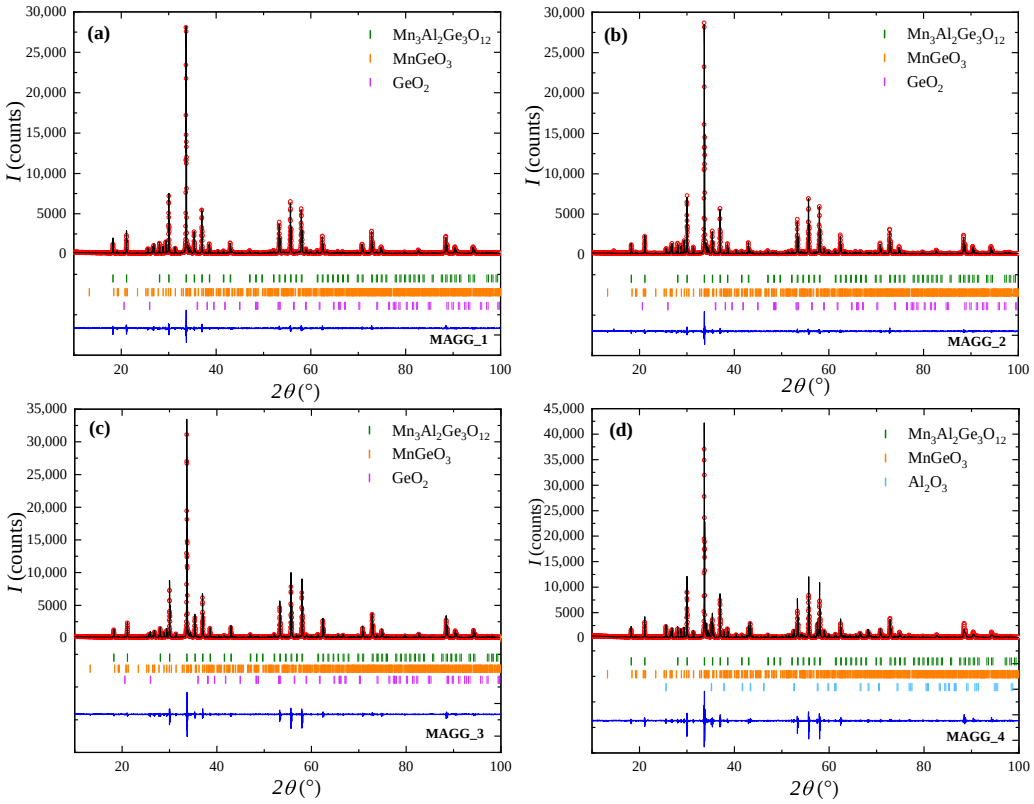

Figure 2. PXRD profiles of four of the polycrystalline $Mn_3Al_2Ge_3O_{12}$ samples (labeled MAGG_1, MAGG_2, MAGG_3, and MAGG_4), prepared using different amounts of excess GeO_2. (**a**–**c**) MAGG_1, MAGG_2 and MAGG_3, prepared using 5, 10 and 15% of GeO_2 excess, respectively, in three steps, at 900 °C, 1100 °C, and 1150 °C for 24 h. (**d**) MAGG_4, prepared using 0% GeO_2 excess in three steps, at 900 °C, 1100 °C, and 1150 °C for 48–72 h. The red open circles represent the experimental profiles and the black lines are the calculated profiles, with the difference given by the blue lines. The reflections of the cubic $Mn_3Al_2Ge_3O_{12}$ garnet structure are indicated by green "I" while orthorhombic (*Pbca*) $MnGeO_3$, trigonal ($P3_221$) GeO_2 and rhombohedral ($R\bar{3}c$) Al_2O_3 are represented using orange, pink and light blue "I" respectively.

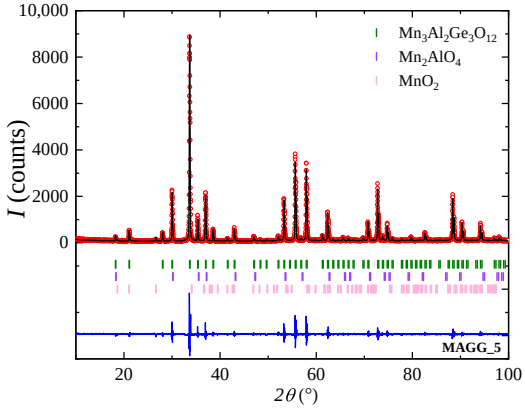

Figure 3. PXRD profile of a $Mn_3Al_2Ge_3O_{12}$ polycrystalline sample (sample labeled MAGG_5), prepared in three steps, at 900 °C, 1100 °C, and 1150 °C for 24 h. The red open circles represent the experimental profile and the black line is the calculated profile, with the difference given by the blue line. The reflections of the $Mn_3Al_2Ge_3O_{12}$ garnet structure are indicated by green "I" while orthorhombic (*Pbca*) MnO_2 and cubic ($Fd\bar{3}m$) Mn_2AlO_4 are represented by the pale pink and purple "I" respectively.

The conditions used for the synthesis of the $Mn_3Al_2Ge_3O_{12}$ polycrystalline materials, as well as the results of the phase composition analysis of each sample, are summarized in Table 1.

Table 1. Summary of the conditions used for the preparation of the $Mn_3Al_2Ge_3O_{12}$ polycrystalline samples. All the samples were sintered in nitrogen gas atmosphere. The results of the phase composition analysis by powder X-ray diffraction are given for each sample.

Sample Label	Synthesis Conditions		GeO_2 Excess (%)	Phase Composition Analysis
	Temperature (°C)	Duration (h)		
MAGG_1	900 1100 1150	24 24 24	5	mixture of cubic $Mn_3Al_2Ge_3O_{12}$, orthorhombic $MnGeO_3$ and trigonal GeO_2
MAGG_2	900 1100 1150	24 24 24	10	mixture of cubic $Mn_3Al_2Ge_3O_{12}$, orthorhombic $MnGeO_3$ and trigonal GeO_2
MAGG_3	900 1100 1150	24 24 24	15	mixture of cubic $Mn_3Al_2Ge_3O_{12}$, orthorhombic $MnGeO_3$ and trigonal GeO_2
MAGG_4	900 1050 1150	48 48 72	0	mixture of cubic $Mn_3Al_2Ge_3O_{12}$, orthorhombic $MnGeO_3$ and rhombohedral Al_2O_3
MAGG_5	900 1100 1150	24 24 24	0	mainly cubic $Mn_3Al_2Ge_3O_{12}$, a few peaks of cubic Mn_2AlO_4 and orthorhombic MnO_2

3.2. Crystal Growth

All the $Mn_3Al_2Ge_3O_{12}$ garnet crystal boules were grown using the floating zone technique in a static nitrogen gas atmosphere, at a pressure of 1–3.5 bars and at a growth rate of 2–20 mm h^{-1}. The two rods (feed and seed) were counter-rotated at a rate of 5–16 rpm. The crystal boules do not appear to melt congruently, and typically, it was observed that higher growth rates help to stabilise the molten zone. Furthermore, a white residue was observed on the quartz tube surrounding the feed and the seed rods. A powder X-ray diffraction analysis of the white residue showed that this residue is GeO_2 [23], suggesting that a small amount of GeO_2 is lost during the crystal growth process due to evaporation.

We have first attempted to grow crystal boules of $Mn_3Al_2Ge_3O_{12}$ using a feed rod prepared with polycrystalline material from a starting powder mixture enriched in germanium (synthesised in the same conditions as the MAGG_3 sample, using 15% excess GeO_2). To suppress the evaporation of GeO_2 during the crystal growth process, the growth was carried out in a nitrogen gas atmosphere, at a pressure of 3–3.5 bars, and using a growth rate of 20 mm h^{-1}. A high growth rate was employed as the molten zone was not stable when lower growth rates were used. The $Mn_3Al_2Ge_3O_{12}$ garnet boule obtained (crystal boule labeled MAGG_C1) was ∼4–5 mm in diameter and ∼55 mm long. The MAGG_C1 boule, pictured in Figure 4, was an orange-red colour and it was opaque. In the first few millimeters (region neighbouring the seed), the boule developed strong facets, however, as the growth progressed, the facets disappeared and multiple tiny facets started developing along the entire length of the crystal boule. X-ray Laue photographs taken of the MAGG_C1 boule revealed a poor crystalline quality. In addition, the PXRD pattern collected on a ground fragment showed the presence of a mixture of phases, the $Mn_3Al_2Ge_3O_{12}$ garnet and an orthorhombic (*Pbca*) $MnGeO_3$ impurity, as can be observed in Figure 4.

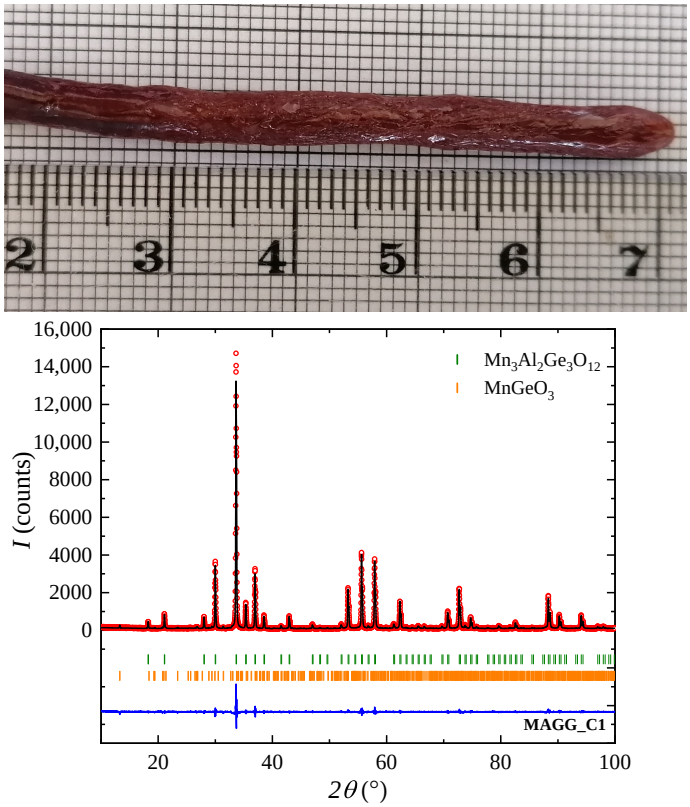

Figure 4. (**top**) As-grown crystal boule of $Mn_3Al_2Ge_3O_{12}$ (sample labeled MAGG_C1) obtained in nitrogen gas atmosphere at a pressure of 3–3.5 bars and using a growth rate of 20 mm h^{-1}. The feed rod was prepared using the starting polycrystalline $Mn_3Al_2Ge_3O_{12}$ with a 15% excess of GeO_2 (same conditions used to synthesize the MAGG_3 sample). (**bottom**) PXRD profile of a ground crystal fragment isolated from the MAGG_C1 boule. The red open circles represent the experimental profile and the black line is the calculated profile, with the difference given by the blue line. The reflections of the $Mn_3Al_2Ge_3O_{12}$ garnet structure are indicated by green "I" while the reflections of the orthorhombic (*Pbca*) $MnGeO_3$ impurity are represented by orange "I".

In a second attempt, crystal boules of $Mn_3Al_2Ge_3O_{12}$ were grown using feed rods prepared using polycrystalline material from a stoichiometric starting mixture (synthesised using the same conditions as the MAGG_5 sample). Initially, a polycrystalline rod was used as a seed, and once a good quality crystal boule was obtained, a crystal seed was used for subsequent growths. The crystal growths were carried out in nitrogen gas atmosphere, at a pressure of ∼1 bar, using a growth rate of 20 mm h^{-1}. A $Mn_3Al_2Ge_3O_{12}$ crystal boule (labeled MAGG_C2) obtained using these growth conditions is shown in Figure 5. The MAGG_C2 boule was ∼4–5 mm in diameter and ∼58 mm long, and appeared to be a black, opaque colour. However, later inspection of thin slices of the crystal of less than 0.7 mm in thickness reveal the crystal to be dark orange in colour. Post-growth annealing on small crystal fragments at 900° for 24 h made no difference to the appearance of either the MAGG_C1 or MAGG_C2 boules. It is worth noting that a minute amount of white residue was observed on the quartz tube surrounding the feed and the seed rod, suggesting that a very small amount of GeO_2 is lost during the crystal growth process,significantly less compared to the other crystal growth attempts. Long, reflective facets were formed along almost the entire length of the crystal boule. X-ray Laue photographs taken of the boule confirm the good crystalline quality of the MAGG_C2 crystal boule. A large single crystal region with good crystalline quality of length 3 cm, as labeled in Figure 5, could be isolated from the crystal boule for subsequent characterization measurements.

Phase purity analysis was carried out on a ground crystal piece of the MAGG_C2 boule, and the powder X-ray diffraction pattern is shown in Figure 6. Profile matching

confirms that the main phase is the $Mn_3Al_2Ge_3O_{12}$ cubic garnet phase, with no significant impurity phases present. The lattice parameter was determined to be a = 11.90479(5) Å, in agreement with previous studies [20].

Composition analysis by EDAX was performed on a cleaved piece from the MAGG_C2 crystal boule. The average atomic percentages of Mn, Al, Ge, and O were 15.1(2)%, 10.5(8)%, 13.8(7)%, and 60.4(3)% respectively. Given the limitations of this technique, the results are in reasonable agreement with the expected theoretical values of 15%, 10%, 15%, and 60% for Mn, Al, Ge, and O respectively. Taking into consideration the results, the chemical composition of the MAGG_C2 crystal boule is $Mn_{3.02}Al_{2.12}Ge_{2.77}O_{12.08}$. This could be a result of a small deviation in the congruent melting composition from the stoichiometric composition and it has been previously reported in other garnets, such as the gadolinium scandium aluminium garnet (GSAG) garnet [39,40].

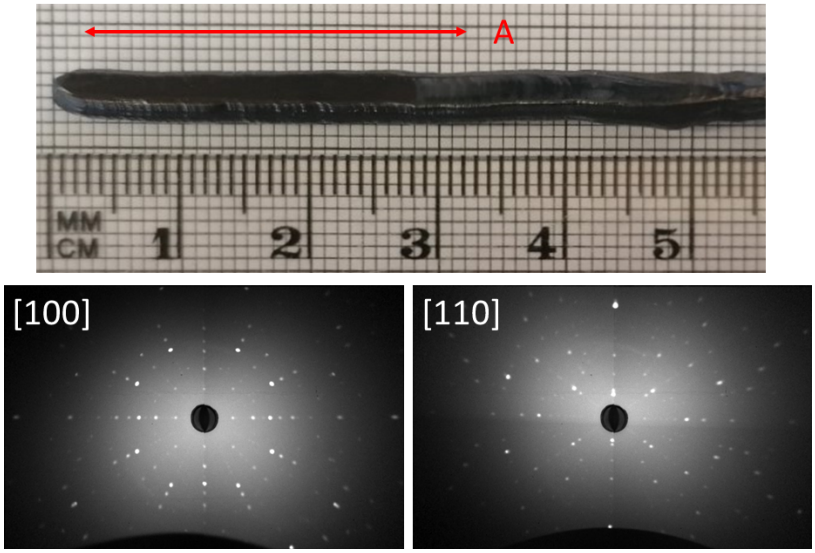

Figure 5. As-grown crystal boule of $Mn_3Al_2Ge_3O_{12}$ (sample labeled MAGG_C2), prepared by the floating zone technique, in nitrogen gas atmosphere, at a pressure of 1 bar, using a growth rate of 20 mm h^{-1} (**top**). A single crystal of ~3 cm length was isolated from the $Mn_3Al_2Ge_3O_{12}$ crystal boule, labeled as region A. Also shown are the X-ray Laue back reflection photographs showing the [100] and [110] orientations of an aligned sample used for magnetic properties measurements (**bottom**).

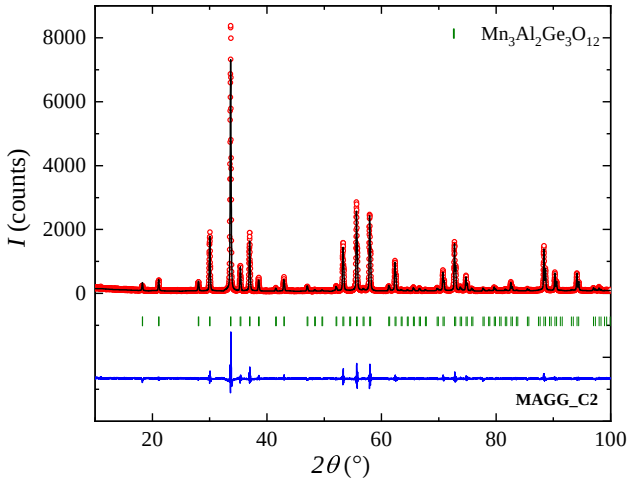

Figure 6. PXRD profile of a ground crystal fragment isolated from the $Mn_3Al_2Ge_3O_{12}$ boule (labelled MAGG_C2). The red open circles represent the experimental profile and the black line shows the calculated profile, with the difference given by the blue line. The reflections of the $Mn_3Al_2Ge_3O_{12}$ garnet structure are indicated by green "|".

The difficulties encountered in stabilising the molten zone prompted us to attempt to a third growth attempt, with the feed rod consisting of a crystal boule prepared using the same parameters as for the growth of MAGG_C2 boule. Typically, premelting of the feed rods is used for the growth of incongruently melting materials, when there are no signs of evaporation [41]. The reduced evaporation observed using the parameters employed to prepare the MAGG_C2 boule suggested that premelting the rods could be a possible solution that could help to stabilise the molten zone at lower growth rates. A crystal boule previously premelted using the same parameters as for the growth of the the MAGG_C2 boule was used as seed rod. The crystal growth was then carried out in nitrogen gas atmosphere, at a pressure of ∼1 bar, using a growth rate of 2–6 mm h^{-1}. Figure 7 shows the resulting crystal boule (labeled MAGG_C3). The MAGG_C3 boule appeared to be a black colour, of a variable diameter due to difficulties encountered in stabilising the molten zone. In addition, a rather large amount of white residue was observed on the quartz tube surrounding the feed and the seed rod. Therefore, the crystal boule obtained was not of good crystalline quality, and a large size single crystal region was not produced, as confirmed by the X-ray Laue backscattering analysis. X-ray Laue photographs are consistent along the length of the 7 mm, labelled B, however, the single crystal region did not extend to the entire width of the boule. Phase composition analysis by powder X-ray diffraction of a ground crystal fragment of the MAGG_C3 boule (see Figure 8) reveals that, although the main phase is the cubic $Mn_3Al_2Ge_3O_{12}$ garnet, there is a small amount of a cubic ($Fd\bar{3}m$) $MnAl_2O_4$ impurity present in the crystal [42]. These results indicate that the crystal growth attempt using a premelted rod was not successful in producing a good quality, pure phase crystal boule due to the loss of GeO_2 during the initial premelting phase and during the crystal growth process.

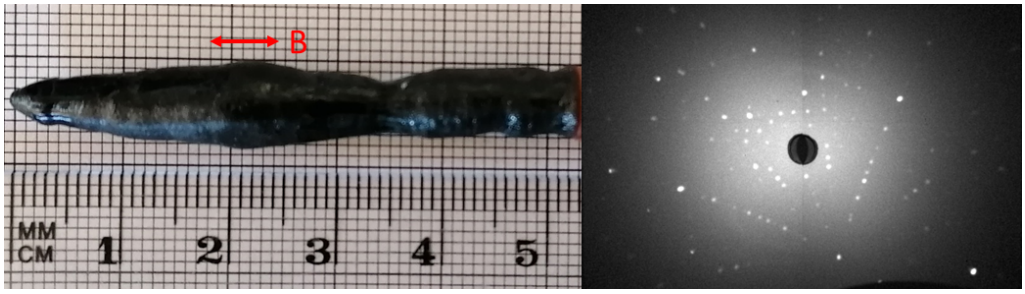

Figure 7. (**left**) As-grown crystal boule of $Mn_3Al_2Ge_3O_{12}$ (sample labeled MAGG_C3) obtained, in nitrogen gas atmosphere at a pressure of 1 bar, by melting the feed rod twice using a growth rate of 2–6 mm h^{-1}. The initial polycrystalline feed rod (prepared in the same conditions as the MAGG_5 sample) was processed at a growth rate of 20 mm h^{-1}. The boule thus obtained was used as feed rod for the final crystal growth, when a growth rate of rate of 2–6 mm h^{-1} was employed. (**right**) The Laue backscattering photograph corresponds to the consistent pattern obtained from the region labeled B, 7 mm in length.

To summarize our attempts to grow $Mn_3Al_2Ge_3O_{12}$ crystal boules by the floating zone method, the best crystals were obtained starting from feed rods obtained using the same synthesis conditions as for the preparation of the MAGG_5 sample. In addition, the growth parameters that allowed us to obtain better quality boules and to isolate a good size single crystal for characterization measurements are the ones used to prepare the MAGG_C2 crystal boule. Furthermore, it is worth noting that the use of a high growth rate helped us to achieve a stable molten zone, and was crucial in obtaining large, good quality single crystals.

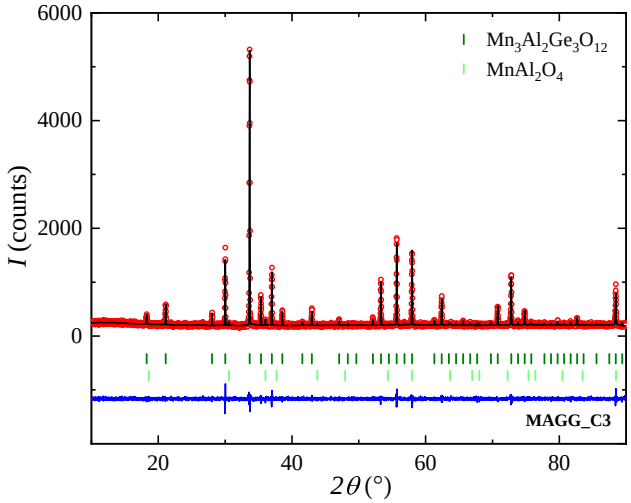

Figure 8. PXRD profile of a ground crystal fragment isolated from the MAGG_C3 boule. The red open circles represent the experimental profile and the black line is the calculated profile, with the difference given by the blue line. The reflections of the $Mn_3Al_2Ge_3O_{12}$ garnet structure are indicated by dark green "|" while the reflections of the cubic ($Fd\bar{3}m$) $MnAl_2O_4$ impurity are represented by light green "|".

A summary of the conditions used for each crystal growth of $Mn_3Al_2Ge_3O_{12}$ garnet is given in Table 2.

Table 2. Summary of the conditions used for the growth of the $Mn_3Al_2Ge_3O_{12}$ garnet crystal boules [a].

Crystal Label	Growth Rate (mm/h)	Gas Atmosphere/ Pressure	Feed & Seed Rotation Rate (rpm)	Remarks
MAGG_C1	20	N_2, 3–3.5 bars	6-6	mainly cubic $Mn_3Al_2Ge_3O_{12}$ phase and a few peaks of orthorhombic $MnGeO_3$
MAGG_C2	20	N_2, 1 bar	10-16	cubic $Mn_3Al_2Ge_3O_{12}$ phase ★ grain $\sim$ 4–5 $\times$ 4–5 $\times$ 30 mm^3
MAGG_C3	2-6	N_2, 1 bar	10-5	mainly cubic $Mn_3Al_2Ge_3O_{12}$ phase and a few peaks of cubic $MnAl_2O_4$

[a] The optimal growth conditions that allowed us to obtain the best quality boule and to isolate a good size single crystal fragment for characterisation measurements are marked using ★.

3.3. Magnetic Characterisation

Magnetisation measurements were performed on a small $Mn_3Al_2Ge_3O_{12}$ single crystal fragment ($5 \times 3 \times 2$ mm^3) of mass 60.8610(5) mg, isolated from the MAGG_C2 boule. The temperature dependence of the *dc* magnetic susceptibility, $\chi(T)$, and the reciprocal, $\chi^{-1}(T)$, in an applied magnetic field of 500 Oe with $H \parallel [100]$ and $H \parallel [110]$ are shown in Figure 9. Consideration of the demagnetisation factor made no significant difference to the results of these measurements and was therefore disregarded and the raw data used.

For both crystallographic directions, the magnetic susceptibility exhibits a monotonic increase when cooling from 300 to 1.8 K, and an anomaly is observed at low temperature. This feature centered around 6.5(1) K suggests the antiferromagnetic ordering of the Mn^{2+} ions, agreeing with previous reports in which the ordering temperature varies between 6.3 K [23] and 6.8 K [19,24–26] for both polycrystalline and single crystal samples. A fit of the $\chi^{-1}(T)$ to a Curie-Weiss law over the temperature range 50–300 K shows that the $Mn_3Al_2Ge_3O_{12}$ garnet has an effective moment of $\mu_{\text{eff}} = 5.7(1)\ \mu_B$ for $H \parallel [100]$ and $\mu_{\text{eff}} = 5.9(1)\ \mu_B$ for $H \parallel [110]$. The effective moment of Mn^{2+} in manganese aluminium germanium garnet is in agreement with the magnetic moment of a free Mn^{2+} ion. The Weiss

temperature of $Mn_3Al_2Ge_3O_{12}$ was also calculated for the two crystallographic directions, and was found to be equal to $\theta_W = -18.5(1)$ K for $H \parallel [100]$ and $\theta_W = -20.7(1)$ K for $H \parallel [110]$. The negative value of the Weiss temperature indicates an antiferromagnetic coupling of the Mn^{2+} ions, however the values obtained differ slightly from the previously reported results of 25 K, for a single crystal sample [23], and 28 K [19], for a polycrystalline sample.

The anisotropy in the magnetic susceptibility, χ, evident in Figure 9 has been observed previously in different crystallographic orientations [23] and has been linked to the relative orientation of the applied magnetic field to the vector normal to the plane of triangular spins in the crystal structure. This has also previously been used to explain the differences in μ_{eff} and θ_W for each crystallographic direction [23].

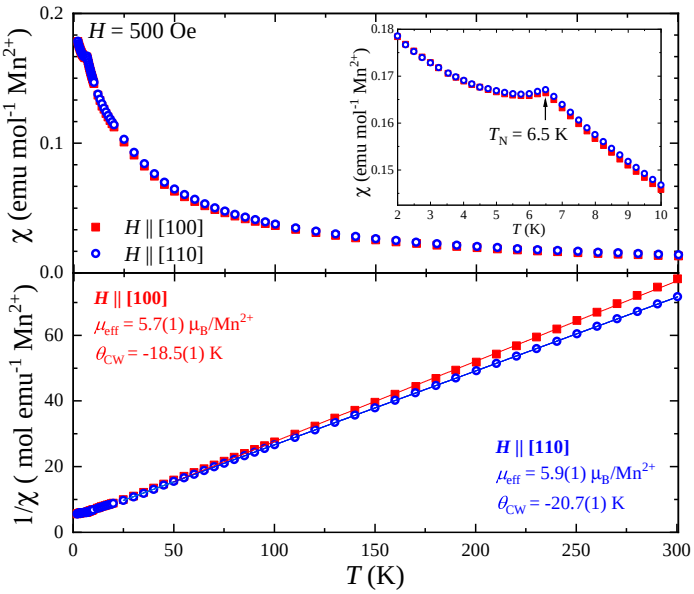

Figure 9. (**top**) Temperature dependent magnetic susceptibility, $\chi(T)$, for a $Mn_3Al_2Ge_3O_{12}$ crystal fragment isolated from the MAGG_C2 boule, for $H \parallel [100]$ (shown in red) and $H \parallel [110]$ (blue), in the temperature range 2−300 K and an applied magnetic field of 500 Oe. The inset shows an ordering temperature of $T_N = 6.5$ K. (**bottom**) The temperature dependence of $\chi^{-1}(T)$ and the fit in the temperature range 50−300 K using the Curie-Weiss law.

4. Conclusions

Samples of $Mn_3Al_2Ge_3O_{12}$ garnet were first prepared in polycrystalline form by the conventional solid state synthesis method. The chemical composition analysis using X-ray diffraction techniques revealed the presence of impurities. We have described various synthesis conditions attempted to improve the quality of the powder samples, including the use of excess GeO_2 to improve the phase purity of the resulting polycrystalline material. Studies to further improve the synthesis conditions are now being carried out to obtain phase pure manganese aluminium germanium garnet in powder form. The polycrystalline material that contained the highest percentage of the required $Mn_3Al_2Ge_3O_{12}$ phase was used as the starting material for the synthesis of single crystals of $Mn_3Al_2Ge_3O_{12}$. The different attempts at the crystal growth of $Mn_3Al_2Ge_3O_{12}$ by the floating zone technique are described where the growth parameters were adjusted to overcome difficulties encountered due to the evaporation of GeO_2, and also the in the stabilisation of the liquid molten zone during growth. We have been successful in growing, for the first time, crystal boules of the manganese aluminium germanium garnet using the FZ method. The quality and composition of the as-grown $Mn_3Al_2Ge_3O_{12}$ boules were investigated using X-ray diffraction techniques. It is worth noting that a high speed growth rate of 20 mm h^{-1} helped to stabilise the molten zone and to reduce the amount of GeO_2 lost through evaporation during the crystal growth process. A large, phase-pure single crystal of 3 cm length was

isolated from the $Mn_3Al_2Ge_3O_{12}$ crystal boule, displaying the best crystalline quality. This crystal fragment is now being used for detailed magnetic properties measurements of this system. The large size and high quality of the crystal suggests that it is a good candidate for further physical characterisation, such as magnetisation measurements and neutron scattering measurements.

Author Contributions: M.I. prepared the polycrystalline material and feed rods with supervision and advice from M.C.H. and M.I. carried out the crystal growth. M.I. carried out X-ray diffraction and magnetic characterisation. M.C.H. performed analysis of the X-ray data. O.A.P. gave supervision and advice on characterisation techniques. M.I. and M.C.H. undertook the original draft preparation and all authors reviewed and edited the manuscript. O.A.P. and G.B. conceived and supervised the project. All authors have read and agreed to the published version of the manuscript.

Funding: Financial support was provided by EPSRC, UK, through Grant EP/T005963/1.

Data Availability Statement: Data is available from the authors upon request.

Acknowledgments: The authors would also like to thank T. E. Orton for valuable technical support, S. J. York for the chemical composition analysis using EDAX, and D. Walker and D. Mayoh for the assistance provided with the PXRD measurements.

Conflicts of Interest: The authors declare no conflict of interest.

Sample Availability: Crystal samples of the compound $Mn_3Al_2Ge_3O_{12}$ are available from the authors.

References

1. Prandl, W. Rhombohedral Magnetic Structure in Spessartite Type Garnets. *Phys. Status Solidi B* **1973**, *55*, K159–K163. [CrossRef]
2. Lau, G.C.; Klimczuk, T.; Ronning, F.; McQueen, T.M.; Cava, R.J. Magnetic properties of the garnet and glass forms of $Mn_3Al_2Si_3O_{12}$. *Phys. Rev. B* **2009**, *80*, 214414. [CrossRef]
3. Geller, S. Crystal chemistry of the garnets. *Z. Krist.-Cryst. Mater.* **2014**, *125*, 1–47. [CrossRef]
4. Deen, P.P. An Overview of the Director State in Gadolinium Gallate Garnet. *Front. Phys.* **2022**, *10*, 868339. [CrossRef]
5. Ramirez, A.P. Strongly Geometrically Frustrated Magnets. *Ann. Rev. Mater. Sci.* **1994**, *24*, 453–480. [CrossRef]
6. Greedan, J.E. Geometrically frustrated magnetic materials. *J. Mater. Chem.* **2001**, *11*, 37–53. [CrossRef]
7. Moessner, R.; Ramirez, A.P. Geometrical frustration. *Phys. Today* **2006**, *59*, 24–29. [CrossRef]
8. Canals, B.; Lacroix, C. Pyrochlore Antiferromagnet: A Three-Dimensional Quantum Spin Liquid. *Phys. Rev. Lett.* **1998**, *80*, 2933–2936. [CrossRef]
9. Kitagawa, K.; Takayama, T.; Matsumoto, Y.; Kato, A.; Takano, R.; Kishimoto, Y.; Bette, S.; Dinnebier, R.; Jackeli, G.; Takagi, H. A spin-orbital-entangled quantum liquid on a honeycomb lattice. *Nature* **2018**, *554*, 341–345. [CrossRef]
10. Bramwell, S.T.; Harris, M.J. The history of spin ice. *J. Phys. Condens. Matter* **2020**, *32*, 374010. [CrossRef]
11. Gardner, J.S.; Gingras, M.J.P.; Greedan, J.E. Magnetic pyrochlore oxides. *Rev. Mod. Phys.* **2010**, *82*, 53–107. [CrossRef]
12. Schiffer, P.; Ramirez, A.P.; Huse, D.A.; Valentino, A.J. Investigation of the Field Induced Antiferromagnetic Phase Transition in the Frustrated Magnet: Gadolinium Gallium Garnet. *Phys. Rev. Lett.* **1994**, *73*, 2500–2503. [CrossRef]
13. Nakamura, T.; Miyashita, S. Thermodynamic properties of the quantum Heisenberg antiferromagnet on the kagomé lattice. *Phys. Rev. B* **1995**, *52*, 9174–9177. [CrossRef] [PubMed]
14. Kuroda, A.; Miyashita, S. Existence of Phase Transition in Ising-like Heisenberg Antiferromagnets on the Kagome Lattice. *J. Phys. Soc. Jpn.* **1995**, *64*, 4509–4512.
15. d'Ambrumenil, N.; Petrenko, O.A.; Mutka, H.; Deen, P.P. Dispersionless Spin Waves and Underlying Field-Induced Magnetic Order in Gadolinium Gallium Garnet. *Phys. Rev. Lett.* **2015**, *114*, 227203. [CrossRef]
16. Paddison, J.A.M.; Jacobsen, H.; Petrenko, O.A.; Fernández-Díaz, M.T.; Deen, P.P.; Goodwin, A.L. Hidden order in spin-liquid $Gd_3Ga_5O_{12}$. *Science* **2015**, *350*, 179–181. [CrossRef] [PubMed]
17. Claudine, L.; Mendels, P.; Mila, F. *Introduction to Frustrated Magnetism*; Springer: Berlin/Heidelberg, Germany, 2011; Volume 164. [CrossRef]
18. Plumier, R. Determination par diffraction des neutrons de la structure antiferromagnetique du grenat $Mn_3Al_2Ge_3O_{12}$. *Solid State Commun.* **1973**, *12*, 109–112. [CrossRef]
19. Valyanskaya, T.V.; Plakhtii, V.P.; Sokolov, V.I. Antiferromagnetism of the garnet $Mn_3Al_2Ge_3O_{12}$. *Sov. Phys. JETP* **1976**, *43*, 1189.
20. Min, J.; Zheng, S.; Gong, J.; Chen, X.; Liu, F.; Xie, Y.; Zhang, Y.; Ma, Z.; Liu, M.; Wang, X.; et al. Magnetoelectric Effect in Garnet $Mn_3Al_2Ge_3O_{12}$. *Inorg. Chem.* **2022**, *61*, 86–91. [CrossRef]
21. Pajaczkowska, A.; Jasiołek, G.; Majcher, K. Crystal growth and some structural investigations of $Mn_3Al_2Ge_3O_{12}$ (MAGG) garnets, where A = Cr, Fe, Ga. *J. Cryst. Growth* **1986**, *79*, 417–420. [CrossRef]
22. Tauber, A.; Banks, E.; Kedesdy, H.H. Magnetic Germanates Isostructural with Garnet. *J. Appl. Phys.* **1958**, *29*, 1123. [CrossRef]

23. Kazei, Z.A.; Kolmakova, N.P.; Levanidov, M.V.; Mill, B.V.; Sokolov, V.I. Magnetoanisotropic properties of the exchange-noncollinear antiferromagnet $Mn_3Al_2Ge_3O_{12}$. *Sov. Phys. JETP* **1987**, *65*, 2277–2282.
24. Krasnikova, Y.V.; Glazkov, V.N.; Soldatov, T.A. Experimental study of antiferromagnetic resonance in noncollinear antiferromagnetic $Mn_3Al_2Ge_3O_{12}$. *JETP* **2017**, *125*, 476–479. [CrossRef]
25. Tikhonov, A.M.; Pavlov, N.G.; Udalov, O.G. Nuclear magnetic resonance in noncollinear antiferromagnet $Mn_3Al_2Ge_3O_{12}$. *JETP Lett.* **2012**, *96*, 517–520. [CrossRef]
26. Gukasov, A.; Plakhty, V.P.; Dorner, B.; Kokovin, S.Y.; Syromyatnikov, V.N.; Smirnov, O.P.; Chernenkov, Y.P. Inelastic neutron scattering study of spin waves in the garnet $Mn_3Al_2Si_3O_{12}$ with a triangular magnetic structure. *J. Phys. Condens. Matter* **1999**, *11*, 2869–2878. [CrossRef]
27. Gardner, J.; Gaulin, B.; Paul, D. Single crystal growth by the floating-zone method of a geometrically frustrated pyrochlore antiferromagnet, $Tb_2Ti_2O_7$. *J. Cryst. Growth* **1998**, *191*, 740–745. [CrossRef]
28. Balakrishnan, G.; Petrenko, O.A.; Lees, M.R.; Paul, D.M. Single crystal growth of rare earth titanate pyrochlores. *J. Phys. Condens. Matter* **1998**, *10*, L723–L725. [CrossRef]
29. Brunt, D.; Ciomaga Hatnean, M.; Petrenko, O.A.; Lees, M.R.; Balakrishnan, G. Single-Crystal Growth of Metallic Rare-Earth Tetraborides by the Floating-Zone Technique. *Crystals* **2019**, *9*, 211. [CrossRef]
30. Balakrishnan, G.; Hayes, T.J.; Petrenko, O.A.; Paul, D.M. High quality single crystals of the SrR_2O_4 family of frustrated magnets. *J. Phys. Condens. Matter* **2008**, *21*, 012202. [CrossRef]
31. Rodríguez-Carvajal, J. Recent advances in magnetic structure determination by neutron powder diffraction. *Phys. B Condens. Matter* **1993**, *192*, 55–69. [CrossRef]
32. Becker, U.; Felsche, J. Phases and structural relations of the rare earth germanates $RE_2Ge_2O_7$, RE≡La-Lu. *J. Less Common. Met.* **1987**, *128*, 269–280. [CrossRef]
33. Redhammer, G.J.; Senyshyn, A.; Tippelt, G.; Roth, G. Magnetic spin structure of pyroxene-type $MnGeO_3$. *J. Phys. Condens. Matter* **2011**, *23*, 254202. [CrossRef] [PubMed]
34. Herpin, P.; Whuler, A.; Boucher, B.; Sougi, M. Étude cristallographique et magnétique de $MnGeO_3$. *Phys. Status Solidi B* **1971**, *44*, 71–84.
35. Finch, C.B.; Clark, G.W. Flux growth and characterization of hexagonal germanium dioxide single crystals. *Am. Mineral.* **1968**, *53*, 1394–1398.
36. Lewis, J.; Schwarzenbach, D.; Flack, H.D. Electric field gradients and charge density in corundum, α-Al_2O_3. *Acta Crystallogr. A* **1982**, *38*, 733–739.
37. Dekker, E.H.L.J.; Rieck, G.D. Revised phase diagram and X-ray data of the $Mn_3O_4Al_2O_3$ system in air. *Z. Anorg. Allg. Chem.* **1975**, *415*, 69–80.
38. Kedesdy, H.; Katz, G.; Levin, S.B. Structural relationship between ramsdellite and some synthetic manganese dioxides. *Acta Crystallogr.* **1957**, *10*, 780–781.
39. Lutts, G.B.; Denisov, A.L.; Zharikov, E.V.; Zagumennyi, A.I.; Kozlikin, S.N.; Lavrishchev, S.V.; Samoylova, S.A. GSAG and YSAG: a study on isomorphism and crystal growth. *Opt. Quantum Electron.* **1990**, *22*, S269–S281. [CrossRef]
40. Kaurova, I.; Domoroshchina, E.; Kuz'micheva, G.; Rybakov, V. Evaluation of stability region for scandium-containing rare-earth garnet single crystals and their congruent-melting compositions. *J. Cryst. Growth* **2017**, *468*, 452–456. [CrossRef]
41. Dabkowska, H.; Dabkowski, A. Crystal Growth of Oxides by Optical Floating Zone Technique. In *Springer Handbook of Crystal Growth*; Dhanaraj, G., Byrappa, K., Prasad, V., Dudley, M., Eds.; Springer: Berlin/Heidelberg, Germany, 2010; pp. 367–391.
42. Navarro, R.; Gomez, A.; de Avillez, R. Heat capacity of stoichiometric Al_2MnO_4 spinel between 2 and 873 K. *CALPHAD* **2012**, *37*, 11–17. [CrossRef]